

# Boundary and Symmetry Breaking in a Deformed Toric Code

Rodrigo Corso B. Santos

*Departamento de Física, Universidade Estadual de Londrina*

*Caixa Postal 10011, 86057-970, Londrina, PR, Brasil.\**

This work explores a deformation of Kitaev’s toric code that induces a phase transition out of the topologically ordered phase. By placing the model on a cylinder, the bulk global 1-form symmetries separate into distinct boundary operators, allowing us to show that the transition is accompanied by spontaneous breaking of one higher-form symmetry. Using a holographic (1+1)-dimensional boundary Hamiltonian, we extract an effective central charge and find a pronounced suppression near  $\beta_c$ , followed by its restoration at strong coupling, indicating sensitivity to bulk criticality rather than topological order.

## I. INTRODUCTION

Many strongly correlated quantum systems exhibit topological order, a form of organization not captured by any local order parameter. For example, fractional quantum Hall states have long-range entanglement and a ground-state degeneracy that cannot be lifted by any local perturbation. Such topologically ordered phases may host exotic fractionalized excitations and are intrinsically robust to local noise, a property that has motivated proposals for decoherence-resistant quantum memories and fault-tolerant quantum computation. By its very nature, these phases lie beyond the Landau paradigm: they are characterized by nonlocal entanglement and global properties of the ground state wave function rather than local symmetry-breaking.

Unlike 0-form symmetry-broken phases described by the Landau-Ginzburg-Wilson framework, topologically ordered phases are best understood in terms of their entanglement structure. The hallmark of such order is a finite, universal correction to the topological entanglement entropy, which captures the presence of long-range quantum correlations. Equivalently, topological order may be diagnosed by the existence of non-contractible Wilson and ’t Hooft loops obeying nontrivial algebraic relations, whose expectation values follow area or perimeter laws depending on the phase. These loop operators define higher-form symmetries, generalized symmetries defined by extended objects rather than point-like fields. In two spatial dimensions, a 1-form symmetry acts as a closed loop and its spontaneous breaking directly signals the presence of topological order. This

---

\* rodrigocorso@uel.br

perspective, developed in recent years, unifies gauge-theoretic, categorical, and condensed-matter descriptions of topological phases [1–4].

An archetypal example is Kitaev’s toric code model, an exactly solvable spin Hamiltonian on a two-dimensional lattice [5]. The toric code realizes a  $\mathbb{Z}_2$  topologically ordered phase. Its ground state degeneracy depends on the genus of its manifold, as it supports two species of anyonic quasi-particles (often called “electric” and “magnetic” charges) with mutual anticommutation. Crucially, these anyons and the ground-state degeneracy are protected by the model’s symmetry structure and are robust against local perturbations. Such property forms the basis for topological quantum error correction and fault-tolerant quantum computation. As such, the toric code serves as both a pedagogical prototype and a building block for more intricate topological systems, from string-net models to stabilizer codes and Majorana-based qubits.

A natural question is how this long-range entanglement can be dissolved as one drives the system into a trivial phase. A well-studied example is the deformation introduced in [6], which depends on a perturbation parameter  $\beta$ . For  $\beta = 0$ , one recovers the Kitaev toric code, while as  $\beta$  increases the state continuously approaches a magnetized product state. Remarkably, this model remains exactly solvable for all  $\beta$ . Its analysis shows that the topological entanglement entropy stays at the toric-code value until a critical  $\beta_c$ , where it abruptly drops to zero [6], a signal that the system undergoes a phase transition from a topologically ordered phase to a trivial phase. This model has been used to study anyon condensation and confinement, as  $\beta$  increases certain anyons condense and the phase loses its topological order [7].

Crucially, the deformed toric code model reveals an interesting scenario for a topological-trivial transition. Unlike more familiar transitions between different topological phases (often mediated by anyon condensation/confinement) or transitions involving a conventional symmetry breaking, here it is between a topological phase and a completely trivial phase.

The study of boundaries provides additional insight. A system with topological order in the bulk generally supports gapless, topologically nontrivial boundary modes. The corresponding edge theories often realize conformal field theories (CFTs) whose central charges encode the underlying topological data. In the undeformed toric code, the boundary degrees of freedom map to the Ising CFT with  $c = 1/2$ , reflecting the  $\mathbb{Z}_2$  structure of the bulk. Our main interest here is to investigate such toric code deformation in the presence of an open boundary.

This work is organized as follows. Section II presents the model of study and discusses its main features and points of interest. Section III considers the model in a cylinder and examines the boundary condensing phase structure that arises when we place the model in an open manifold.

Section IV approaches the phase transition from the spontaneous symmetry breaking of a bulk, global 1-form symmetry. At last, in Section V we discuss the holographic correspondence between the bulk and the boundary.

## II. THE MODEL

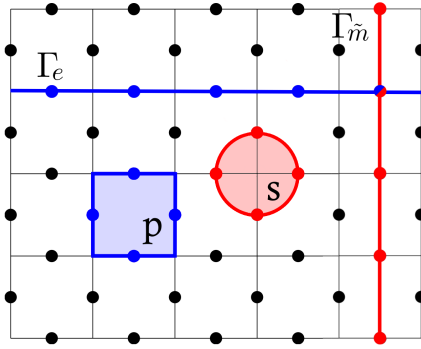


FIG. 1. Electric and magnetic degrees of freedom on the toric code, color online.

In this section we review some of the important aspects of our particular deformation of interest [6]. Like the standard toric code [5], the deformation can be defined in any graph  $G$ . For simplicity we restrict ourselves to the simplest case of a square lattice, where on each link we place a spin-1/2 variable, see Fig. 1. For this review section, we will initially assume periodic boundary conditions (PBC), but later on this will be relaxed to study the effect of the deformation on open boundaries. The Hamiltonian for the deformed toric code (DTC) is given by

$$H_{blk} = \mathcal{J}_p \sum_p (1 - B_p) + \mathcal{J}_s \sum_s e^{-\frac{\beta}{2} \sum_{i \in s} Z_i} (1 - A_s) e^{-\frac{\beta}{2} \sum_{i \in s} Z_i}, \quad (1)$$

where the operators  $B_p = \prod_{i \in p} Z_i$  and  $A_s = \prod_{i \in s} X_i$  are defined as the product of Pauli matrices  $Z$  and  $X$  over edges of plaquettes ( $p$ ) and stars ( $s$ ), as in Fig. 1. One may notice that the deformation only affects the star operators, since it trivially commutes with the plaquette operators.

In fact, the addition of the deformation spoils the commuting projector structure of the original model, since the star operators do not commute with the deformation. Nonetheless, we are still able to find the ground states in a systematic way. The deformed star operators are positive semi-definite as a result of the relation

$$H_s(\beta) = e^{-\frac{\beta}{2} \sum_{ij \in s} Z_{ij}} (1 - A_s) e^{-\frac{\beta}{2} \sum_{ij \in s} Z_{ij}}. \quad (2)$$

$$H_s^2(\beta) = \cosh \left( \beta \sum_{ij \in s} Z_{ij} \right) H_s(\beta). \quad (3)$$

From which we immediately see that the eigenvalues of  $H_s$  must be positive, and therefore, it suffices to look for a state that is annihilated by all the  $H_s$  operators. This is accomplished by the following set of states

$$|GS(\beta)\rangle \propto S(\beta) \prod_s (1 + A_s) |\uparrow\rangle \quad (4)$$

where  $|\uparrow\rangle$  is the fully magnetized state and the deformation  $S(\beta) = \exp\left((\beta/2) \sum_{ij} Z_{ij}\right)$ . In fact, the ground states in (4) belong to a more general class of wavefunctions known as *square root states* [8], which were first observed in the context of a generalization of Rokhsar-Kivelson Hamiltonians and connection to classical Markovian dynamics [9].

Nonetheless, the ground state (4) is not the only ground state of the model. In fact, for periodic boundary conditions the DTC Hamiltonian hosts two higher-form, non-contractible loop symmetries, see Fig. 1. The electric,  $\Gamma_{e,\gamma} = \prod_{\vec{r} \in \gamma} X_{\vec{r}}$  is a traditional symmetry: it is an unitary operator that commutes with the Hamiltonian (1). On the other hand,  $\tilde{\Gamma}_{m,\gamma^*} = S(\beta) \left[ \prod_{\vec{r} \in \gamma^*} X_{\vec{r}} \right] S(\beta)^{-1}$  only commutes with the Hamiltonian when acting on the ground state. Furthermore, in general it is not a unitary operator, a subject we discuss shortly.

As the symmetry operators along different directions on the torus do not commute,

$$\Gamma_{e,\gamma} \tilde{\Gamma}_{m,\gamma^*} = (-1)^{\text{link}(\gamma, \gamma^*)} \tilde{\Gamma}_{m,\gamma^*} \Gamma_{e,\gamma}, \quad (5)$$

the ground states cannot be simultaneously diagonalized by both symmetry operators. This scheme is often referred to as a t'Hooft anomaly and leads to the spontaneous breaking of one of the higher form symmetries and the topological degeneracy of the model [10]. On the torus, there are four topologically distinct ground states

$$|GS; \omega_x, \omega_y\rangle = \frac{1}{\sqrt{\mathcal{Z}_{\omega_x, \omega_y}}} S(\beta) (\Gamma_{m,x})^{\omega_x} (\Gamma_{m,y})^{\omega_y} \sum_s (1 + A_s) |\uparrow\rangle, \quad (6)$$

where  $\omega_{x,y} = 0, 1$  indicates the absence or presence of a non-contractible loop in the  $x$  or  $y$  direction along the torus. Furthermore,  $\Gamma_{m,x} \equiv \tilde{\Gamma}_{m,x}(\beta = 0)$  is the non-deformed magnetic non-contractible loop in the  $x$  direction of the torus. These ground states are graded by the action of the electric symmetries

$$\Gamma_{e,x} |GS; \omega_x, \omega_y\rangle = (-1)^{\omega_y} |GS; \omega_x, \omega_y\rangle \quad \text{and} \quad \Gamma_{e,y} |GS; \omega_x, \omega_y\rangle = (-1)^{\omega_x} |GS; \omega_x, \omega_y\rangle, \quad (7)$$

and the magnetic symmetry is spontaneously broken, such that it maps between the topologically distinct ground states

$$|GS; \omega_x, \omega_y\rangle = \left( \frac{\mathcal{Z}_{0,0}}{\mathcal{Z}_{\omega_x, 0}} \right)^{\omega_x/2} \left( \frac{\mathcal{Z}_{0,0}}{\mathcal{Z}_{0, \omega_y}} \right)^{\omega_y/2} (\tilde{\Gamma}_{m,x})^{\omega_x} (\tilde{\Gamma}_{m,y})^{\omega_y} |GS; 0, 0\rangle. \quad (8)$$

We can get some intuition from these ground states by recasting them in the  $\mathbb{Z}_2$  gauge theory language [11–14], where the ground state of  $H(0)$  can be simply interpreted as the equal weight superposition of all closed loops generated by the action of the product of star operators  $A_s$ . Then the operator  $S(\beta)$  acts on  $|GS(0)\rangle$  it produces a different weight to each state in the superposition. Since the presence of a closed loop makes the eigenvalues of some  $Z$ -operators flip to  $-1$ , the weight of the exponential factor is decreased for large loop configurations.

In this way, the  $\beta$  deformation introduces tension for the loop strings, which has the effect of suppressing large loop configurations, leading to a confined phase. From this analysis, we can already preclude that the model goes through a phase transition at some critical value  $\beta_c$ . For  $\beta < \beta_c$ , the string tension of the loops is not large, and we sit at a deconfined phase (topological order), while for  $\beta > \beta_c$  large loops start to be suppressed, leading to a confined phase, culminating in a trivial product state in the  $\beta \rightarrow \infty$  limit. Recently, the authors in [15] defied this picture, arguing that there may be a gapless regime in between the confined/deconfined phases. We will soon comment more on this subtle point.

Indeed, the DTC is known to undergo a phase transition at  $\beta = \beta_c \equiv \frac{1}{2} \ln(1 + \sqrt{2})$  [6]. This was first unveiled as the topological entanglement entropy suddenly jumps from the toric code topological order value, to zero. This presents a curious kind of phase transition, from a topologically ordered phase to a topologically trivial phase, without explicitly breaking any symmetry of the torus Hamiltonian.

In this representation, the normalization factors  $\mathcal{Z}_{\omega_x, \omega_y}$  can be interpreted in a simple fashion. They are the partition functions of the classical Ising model in two spatial dimensions at inverse temperature  $\beta$ . This is made more explicitly once we make the identification  $Z_{ij} = \theta_{i-1/2,j} \theta_{i+1/2,j}$ , where  $\theta_{i\pm 1/2,j}$  are classical Ising variables located at the vertices bounding the spin  $Z_{i,j}$ .

This mapping leads to an important relation between the quantum DTC and the classical Ising model. The action of a single star operator  $A_s$  on the sum (6) can be encoded on the Ising model by flipping the Ising variable on the same vertex. Then, the sum over all loop configurations on the toric code can be encoded by a sum over Ising configurations. A detailed discussion on this connection can be found in [6, 7]. This equivalence enables the calculation of the expected values of two types of operators. First, for general functions of  $Z$

$$\langle f(Z_{ij}) \rangle_{DTC} = \langle f(\theta_{i-1/2,j} \theta_{i+1/2,j}) \rangle_{Ising}. \quad (9)$$

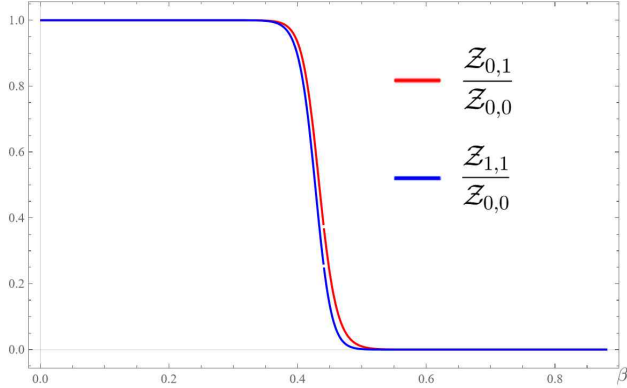


FIG. 2. Ratio of the partition functions against the coupling  $\beta$ .

Additionally, a similar relation holds for the product of  $X_{i,j}$  along a closed path

$$\begin{aligned} \langle \prod_{\gamma^*} X_{i,j} \rangle_{TC} &= \frac{1}{2^{N/2} \sqrt{\mathcal{Z}_{0,0}}} \langle 0, 0 | \left( \prod_{\gamma^*} e^{-\beta Z_{i,j}} \right) S(\beta) \left( \prod_{\gamma^*} X_{i,j} \right) \prod_s (1 + A_s) | \uparrow \rangle \\ &= \langle \prod_{\gamma^*} e^{-\beta Z_{i,j}} \rangle \Rightarrow \langle e^{-\beta \sum_{i,j \in \gamma^*} \theta_{i-1/2,j} \theta_{i+1/2,j}} \rangle_{Ising}. \end{aligned} \quad (10)$$

This connection between the these two models was instrumental in the detection of the critical point in [6]. Furthermore, it also allows us to effectively compute expected values in the DTC ground states by mean values in the classical Ising model at inverse temperature  $\beta$ . While obtaining exact analytical results in the Ising model may be challenging, these quantities may be efficiently estimated using well-established Monte Carlo methods, an approach we adopt in subsequent discussions.

From the mapping between the ground states, equation (8), we see that the ratio between the normalizations can be seen as a measure of the unitarity of the magnetic symmetry on the ground state [7]. See Fig. 2. While  $\tilde{\Gamma}_m$  acts preserving the norm of the ground states up to the critical point, it quickly becomes non-unitarity above  $\beta_c$  and we question whether it truly qualifies as a symmetry of the model.

### III. OPEN BOUNDARY

Topological order in two spatial dimensions manifests not only in the bulk but also through the way the system is terminated. Cutting open one of the non-contractible cycles of the torus introduces decoupled degrees of freedom which, if left ungapped, generate a ground-state degeneracy that scales extensively with system size. To preserve the toric code phase, it is necessary to

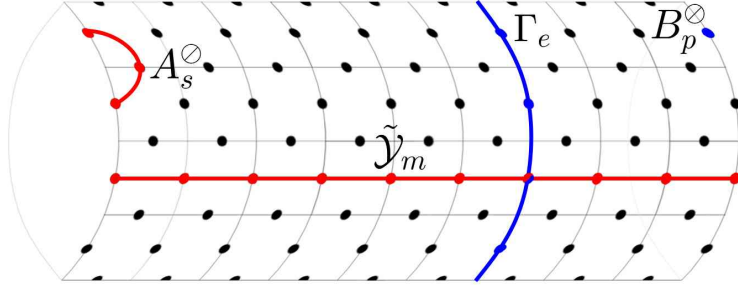


FIG. 3. Smooth boundary on the cylinder.  $B_p^\otimes$  should be thought at just one site.

include in the Hamiltonian boundary operators that gap out these edge degrees of freedom while commuting with the bulk Hamiltonian (1) on the ground-state manifold.

A natural choice for such terms are the incomplete versions of the star and plaquette operators. For the standard toric code ( $\beta = 0$ ), these are the  $A_s^\otimes = \prod_i X_i$  and  $B_p^\otimes = Z$  operators illustrated in Fig. 3. As these boundary operators do not commute between each other, they generate two incompatible boundary phases in the toric code topological ordering. These are characterized by the condensation to the ground state of open strings terminating on the boundary, or equivalently, by the spontaneous breaking of the associated global 1-form symmetries.

The  $\beta$  deformation is introduced in the magnetic sector of the model and is known to destroy the topological order at sufficiently large coupling. Thus, it is natural to question how it affects the condensation scheme and the spontaneous symmetry breaking of the model. To this end, we consider our model on a cylinder, obtained by cutting open one of the directions of the torus. In doing so, the  $\Gamma$  operators running along the different directions in the torus split. We reserve the label  $\Gamma_d$  for the operators running along the periodic direction of the cylinder and  $\mathcal{Y}_d$  for the lines running along the length of the cylinder, as in Fig. 3. The index  $d = \{e, \tilde{m}\}$ .

On the cylinder there are only two degenerate ground states

$$|GS, 0\rangle \quad \text{and} \quad |GS, 1\rangle \propto \mathcal{Y}_d |GS, 0\rangle, \quad (11)$$

which are graded by the  $\Gamma_{d'} |GS, \omega\rangle = (-1)^\omega |GS, \omega\rangle$ , for  $d \neq d'$ . The specific choice of  $d$  and  $d'$  depends on the topological phase of the parent Hamiltonian:  $\mathcal{Y}_d$  already commutes with plaquette and star operators of the bulk Hamiltonian, but only commutes with the incomplete boundary operators of the same “flavor” [1].

The first fixed point Hamiltonian we discuss is produced by the inclusion of the incomplete star

operators  $A_s^\emptyset$  accompanied by the deformation

$$H_{\partial\mathcal{M}}^M = \sum_{s \in \partial\mathcal{M}} e^{-\frac{\beta}{2} \sum_{i \in s} Z_i} (1 - A_s^\emptyset) e^{-\frac{\beta}{2} \sum_{i \in s} Z_i}, \quad (12)$$

The ground states include the all the star operators (complete and incomplete) on the cylinder

$$|\omega\rangle_M = \frac{1}{\sqrt{\mathcal{Z}_\omega}} \left( \tilde{\mathcal{Y}}_m \right)^\omega e^{\frac{\beta}{2} \sum_{i \in \mathcal{M}} Z_i} \prod_{s \in \partial\mathcal{M}} (1 + A_s^\emptyset) \prod_{s \in \mathcal{M}_{blk}} (1 + A_s) |\uparrow\rangle, \quad (13)$$

where  $\omega = 0, 1$ . With the magnetic boundary, the Hamiltonian admits three extended symmetry operators,  $\tilde{\Gamma}_m$ ,  $\Gamma_e$  and  $\tilde{\mathcal{Y}}_m$ . As  $\{\Gamma_e, \tilde{\mathcal{Y}}_m\} = 0$ , the ground state cannot simultaneously diagonalize both symmetries, such that one must be spontaneously broken. While the electric symmetry is diagonal

$$\Gamma_e |\omega\rangle_M = (-1)^\omega |\omega\rangle_M, \quad (14)$$

the magnetic symmetry maps between the two topologically distinct ground states

$$\tilde{\mathcal{Y}}_m |\omega\rangle = \sqrt{\frac{\mathcal{Z}_{\omega+1}}{\mathcal{Z}_\omega}} |\omega+1\rangle. \quad (15)$$

The  $\beta$  deformation affects the condensation scheme for the magnetic boundary. For electric lines ending on the boundary

$$\langle A_s^\emptyset \rangle_M = \begin{cases} 1 & \text{for } \beta = 0 \\ f_m(\beta) & \text{for } \beta \neq 0 \end{cases}, \quad (16)$$

and for magnetic lines

$$\langle B_p^\emptyset \rangle_M = \begin{cases} 0 & \text{for } \beta = 0 \\ f_e(\beta) & \text{for } \beta \neq 0 \end{cases}. \quad (17)$$

While the expected value of the boundary deformed star operator,  $\tilde{A}_s^\emptyset = S(\beta) A_s^\emptyset S^{-1}(\beta)$  remains constant for all beta

$$\langle \tilde{A}_s^\emptyset \rangle_M = 1. \quad (18)$$

In general, states obtained by the action of open lines are excited states. For the boundary fixed point  $H_{\partial\mathcal{M}}^M$ , when the endpoints of a deformed magnetic line are pushed to the boundary, the line operator may be rewritten as a product of complete  $\tilde{A}_s = S(\beta) A_s S^{-1}(\beta)$  and incomplete  $\tilde{A}_s^\emptyset$  deformed star operators. As the ground state (13) is an eigenstate of star operators, the

deformed magnetic excitations condense to the ground state when their endpoints are pushed to the boundary. This is readily seen from by depicting (18) as the superposition between the open line state  $\tilde{A}_s^\emptyset |\omega\rangle_M$  and the ground state  $|\omega\rangle_M$ .

Furthermore, the  $M$  condensation trivializes the action of  $\tilde{\Gamma}_m$ , as it can be written as the product over all  $\tilde{A}_s^\emptyset$ . Conversely,  $\Gamma_e$  cannot be absorbed by the  $M$  condensate, such that it remains a non-trivial symmetry in the low energy limit.

Conversely, we may also produce an electric fixed point Hamiltonian by including the incomplete plaquette operators  $B_p^\emptyset = Z_i$ , as in Fig. 3

$$H_{\partial\mathcal{M}}^E = \sum_{p \in \partial\mathcal{M}} (1 - B_p^\emptyset). \quad (19)$$

For such case, the degenerate ground states include only the bulk star operators

$$|\pm\rangle_E = \frac{1}{\sqrt{\mathcal{Z}_\pm}} e^{\frac{\beta}{2} \sum_{i \in \mathcal{M}_{blk}} Z_i} (1 \pm \Gamma_m) \prod_{s \in \mathcal{M}_{blk}} (1 + A_s) |\uparrow\rangle. \quad (20)$$

They are graded by the magnetic symmetry operator

$$\tilde{\Gamma}_m |\pm\rangle_E = \pm |\pm\rangle_E, \quad (21)$$

and spontaneously break the electric symmetry

$$\mathcal{Y}_e |\pm\rangle_E = |\mp\rangle_E. \quad (22)$$

Furthermore, they are trivially invariant under  $\Gamma_e |\pm\rangle = |\pm\rangle$ .

For this boundary Hamiltonian, the expected value of the boundary operators remain constant for all  $\beta$

$$\langle \tilde{A}_s^\emptyset \rangle_E = 0, \quad \text{and} \quad \langle B_p^\emptyset \rangle_E = 1. \quad (23)$$

The electric boundary Hamiltonian condenses open electric lines with endpoints in a boundary. This can easily seen by observing that these lines can be written as a product complete and incomplete plaquette operators. In contrast, open magnetic lines lead to excited states.

The two boundary Hamiltonians do not commute, but they do commute with the bulk Hamiltonian. In this way, they compete to form two different boundary phases in the toric code topological ordering, such that we study phase transitions via a general Hamiltonian

$$H = H_{blk} + J_p H_{\partial\mathcal{M}}^E + J_s H_{\partial\mathcal{M}}^M. \quad (24)$$

At  $\beta = 0$ , the toric code undergoes a phase transition between the magnetic and electric boundaries at  $J_s = J_p$ . At this point, the boundary becomes gapless as it realizes an Ising criticality.

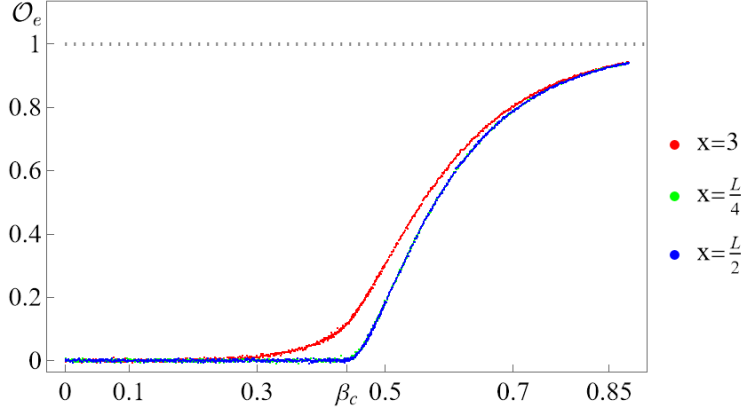


FIG. 4. Order parameter  $\mathcal{O}_e(\beta)$  for  $L = 64$  on a square lattice for the  $|0\rangle$  ground state with varying line distance. Notice that the green and blue points are almost coincident.

#### IV. SYMMETRY BREAKING

The toric code ( $\beta = 0$ ) phase transition is associated with the spontaneous breaking of its *global* 1-form symmetries. At the  $J_p = 0$  fixed point, while  $\Gamma_e$  remains a symmetry of the ground state,  $\tilde{\mathcal{Y}}_m$  is spontaneously broken, as it maps between the two topologically distinct ground states, see equation (15). The symmetry roles are reversed as we cross the  $J_s = J_p$  phase transition. At the  $J_s = 0$  fixed point, while  $\tilde{\Gamma}_m$  is a true symmetry,  $\mathcal{Y}_e$  is spontaneously broken. This scheme guarantees that in either phase, there is always a 1-form symmetry that is spontaneously broken and one that is not. Combined with the electromagnetic duality, this symmetry structure is fundamental in the realization of topological phases and their long range entanglement [1, 16–20].

In general, this 1-form symmetry breaking picture is accompanied by the condensation of boundary anyons. Let us take the magnetic boundary as an example. This fixed point is achieved by the inclusion of magnetic boundary operators to the Hamiltonian, thus, magnetic open lines commute with the Hamiltonian and magnetic degrees of freedom condense to the ground state. As the Hamiltonian contains magnetic boundary terms, it commutes with  $\mathcal{Y}_m$  and not  $\mathcal{Y}_e$ , and the topological states differ by the action of  $\mathcal{Y}_m$ . Furthermore, the two ground states are graded by some non-local symmetry operator that anticommutes with  $\mathcal{Y}_m$ , which leads to  $\Gamma_e$ .

For this boundary, while  $\Gamma_m$  is trivial symmetry,  $\mathcal{Y}_m$  and  $\Gamma_e$  are in a 't Hooft anomaly, leading to the two fold ground state degeneracy. Conversely,  $\mathcal{Y}_e$  is not a symmetry at all.

Turning on the  $\beta$  deformation greatly affects this symmetry breaking structure. Firstly, the expectation values presented in equations (16) and (17) indicate that the condensation pattern is

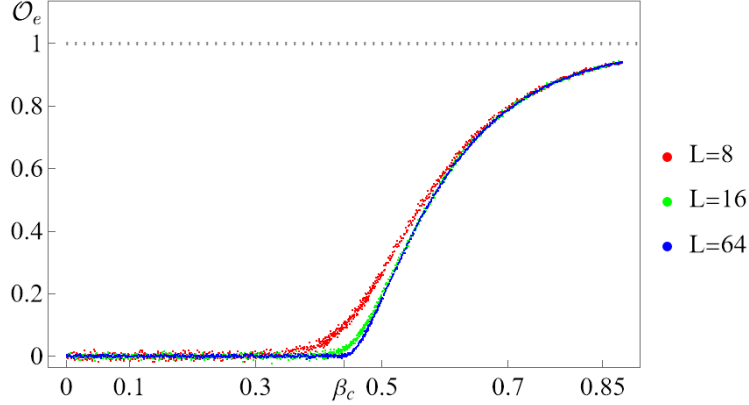


FIG. 5. Order parameter at fixed separation  $x = L/2$  and varying system size  $L = 8, 16, 64$  for a square lattice.

affected by the  $\beta$  deformation. Furthermore, the mapping between the ground states,

$$\tilde{\mathcal{Y}}_m |\omega\rangle = \sqrt{\frac{\mathcal{Z}_{\omega+1}}{\mathcal{Z}_\omega}} |\omega+1\rangle, \quad (25)$$

becomes non-unitary as  $\mathcal{Z}_1/\mathcal{Z}_0 \rightarrow 0$  for  $\beta > \beta_c$ , see Fig. 2. On these grounds, we study the symmetry spontaneous breaking/anyon condensation as a driving of phase transition through the order parameter

$$\mathcal{O}_e = \langle \mathcal{Y}_e(x) \mathcal{Y}_e(0) \rangle, \quad (26)$$

which signals the spontaneous breaking of the global 1-form  $\tilde{\Gamma}_m$  whenever  $\mathcal{O}_e \neq 0$  for large separation  $x$  [21, 22].

Directly computing this order parameter from the deformed toric code ground state is a challenging task. For this reason, we are urged to make use of the mapping between expected values in the deformed toric code and thermal mean values in the Ising model described in equations (9) and (10). With this connection at hand, we are able to effectively simulate the order parameter using a populational Monte Carlo method [23, 24]. This method is specially well suited to our applications as it considers the normalized contributions from the most important loops in the ground state sum to the order parameter.

The resulting estimator for the order parameter can be found in Fig. 4 and 5. Above the critical coupling,  $\beta_c \approx 0.44$ ,  $\mathcal{O}_e \neq 0$  indicating that the remaining magnetic symmetry operator  $\tilde{\Gamma}_m$  is not a symmetry of the ground states. As such, the degenerate ground states are distinguishable by  $\langle \mathcal{Y}_e \rangle$ , as is shown in Fig. 6.

This is fundamentally different from the usual toric code electric-magnetic phase transition. In the non-deformed model, the two phases are connected by a 0-form symmetry. Such that, as we

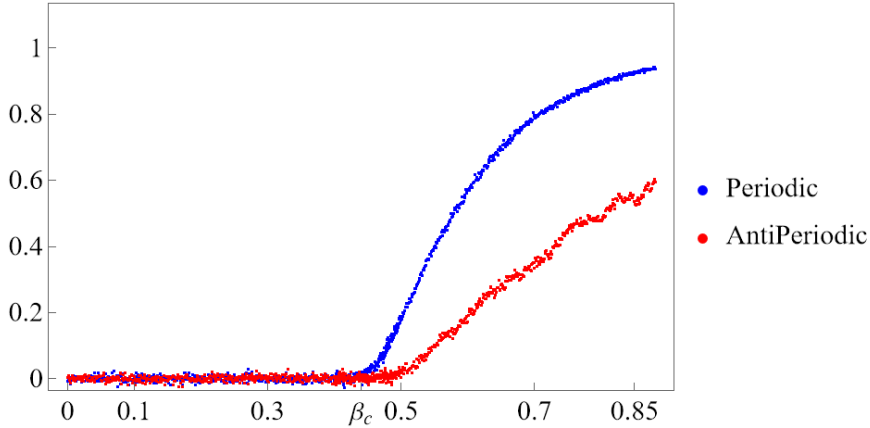


FIG. 6. Vacuum expected value  $\langle \mathcal{Y}_e \rangle$  on the two degenerate ground states for  $L = 32$ .

cross the self-dual  $J_s = J_p$  critical point the roles played by the electric and magnetic symmetry are simply reversed. This process does not change the global symmetry structure of the toric code, such that we may simply exchange the labels  $e \Leftrightarrow m$ .

The symmetry structure consisting of two mutually 't Hooft anomalous 1-form symmetries, tied together by a global electromagnetic 0-form symmetry, stabilizes the toric code topological order and underlies many of its defining properties. In particular, the ground state degeneracy on nontrivial manifolds is a direct manifestation of the 't Hooft anomaly between electric and magnetic line operators, while the nontrivial quantum dimensions of the anyons account for the finite topological entanglement entropy.

Upon crossing the critical point  $\beta_c$  on the magnetic boundary, the magnetic symmetry is greatly degraded:  $\tilde{\Gamma}_m$  is no longer a symmetry of the ground state and  $\tilde{\mathcal{Y}}_m$  becomes nonunitary and, also undermining its interpretation as a bona fide symmetry generator, even if spontaneously broken. Furthermore, since the electromagnetic symmetry exchanges  $e \leftrightarrow m$ , and the electric line operators are insensitive to the  $\beta$  deformation, the electromagnetic symmetry itself must be affected in a nontrivial manner. We argue that this degradation of the intertwined higher-form symmetry structure is the primary mechanism driving the destruction of toric code topological order, as reflected in the vanishing of the topological entanglement entropy for  $\beta > \beta_c$ .

## V. BOUNDARY THEORY

In this section, we investigate the bulk topological phase transition from the perspective of a holographic boundary theory. For both boundaries,  $\Gamma_d$  are topological symmetry operators of the Hamiltonian. As such, we may transport this line to act only on the boundary degrees of

freedom by the action of bulk plaquette and star operators. We may construct a holographic (lower dimensional) Hamiltonian by considering only the spins of the complete (2+1) dimensional Hamiltonian (24) located at the boundary. As  $\Gamma_d$  is topological and the product of local operators, it is also a global symmetry of the holographic Hamiltonian. In this way, we investigate the bulk higher-form symmetry breaking phase transition using a holographic boundary theory as a proxy [1, 4, 22, 25].

The holographic Hamiltonian is obtained by taking only the spins positioned along one of boundaries of the Hamiltonian (24), this yields the holographic, (1+1) dimensional Hamiltonian

$$\begin{aligned} H_{hol} &= J_p \sum_i (1 - Z_i) + J_s \sum_i \left( e^{-\beta(Z_i + Z_{i+1})} - X_i X_{i+1} \right), \\ &\propto -(y + \sinh 2\beta) \sum_i Z_i - \sum_i X_i X_{i+1} \\ &\quad + \sinh^2(\beta) \sum_i Z_i Z_{i+1}, \end{aligned} \tag{27}$$

where  $y \equiv J_p/J_s$ .

In general, a bulk (2+1)-dimensional topological order admits gapless degrees of freedom on the boundary, often being described by a CFT [1, 26–28]. In the usual toric code,  $\beta = 0$ , the holographic Hamiltonian is the transverse field Ising model, which realizes the  $c = 1/2$  Ising CFT by tuning  $y = 1$  [29]. In such case, as we cross the  $y = 1$  critical point the model undergoes a topological phase transition from the toric code’s electric to the magnetic condensing phases. Likewise, its topological boundary transitions from a ferromagnetic to a paramagnetic phase.

A first, naive, analysis might assume the  $Z_i Z_{i+1}$  interaction to be irrelevant in the thermodynamic limit. Under a Jordan-Wigner transformation, such term maps to  $-\gamma_i \gamma'_i \gamma_{i+1} \gamma'_{i+1}$ , which is irrelevant in the low-energy limit by a simple power counting. These considerations would reduce our analysis to the transverse field Ising model with a different parametrization. The boundary would undergo a phase transition whenever the coefficients of the  $Z_i$  and  $X_i X_{i+1}$  terms are equal:

$$y = 1 - \sinh 2\beta, \tag{28}$$

which is the blue plot in Fig. 7. At this critical line the model would host a Kramers-Wannier symmetry, which is inherited from the bulk electromagnetic duality.

The bulk electromagnetic duality constrains the theory even when such marginal operators are neglected, such that this naive analysis reveals the bulk critical point. The boundary parameter  $y$  is restricted to be positive as the bulk requires  $J_p$  and  $J_s$  to be positive, to produce the correct boundary loop condensations. For  $\beta > \beta_c \approx 0.441$  there is no setting of the boundary parameter

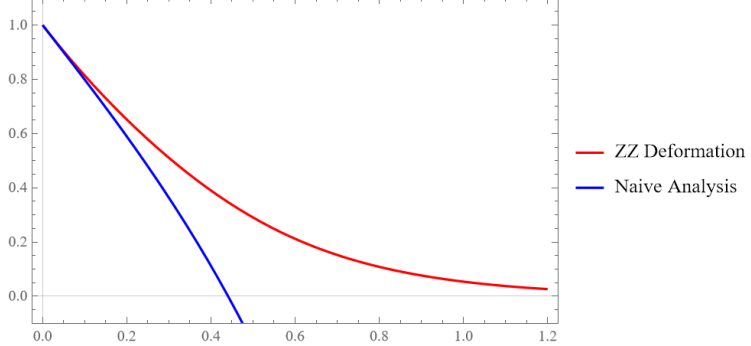


FIG. 7. Critical lines with and without the  $Z_i Z_{i+1}$  term.

$y$  that fully hosts the bulk electromagnetic symmetry, since the bulk is in an electric condensing phase.

In spite of the naive analysis, the  $Z_i Z_{i+1}$  deformation is known to induce non-trivial effects [30–33]. Firstly, such term may be seen as a dynamical mechanism for mass generation by giving an expected value for  $Z_i$ . This displaces the critical line away from the naive analysis (28). Beyond this perturbative argument, the full holographic Hamiltonian admits a non-perturbative identification with the next-nearest-neighbor Ising (ANNNI) model, for which the ferromagnetic-paramagnetic phase transition is known to be at

$$1 - \frac{2U}{\Delta} = \frac{1}{\Delta} - \frac{U}{2\Delta^2(\Delta - U)}, \quad (29)$$

for  $\Delta \equiv y + \sinh 2\beta$  and  $U \equiv \sinh^2 \beta$ . The critical line in terms of the variables most natural to our problem  $y(\beta)$  is depicted in red in Fig. 7.

For small  $\beta$  the  $ZZ$  deformation is still small and we may tune  $y$  such that the  $c = 1/2$  Ising criticality survives, indicating that the bulk toric code topological order is also present for small  $\beta$ . Conversely, for greater values of  $\beta$ , the  $ZZ$  deformation produces more subtle effects. At the critical line, we may recast our model as a  $T\bar{T}$  deformation of the transverse field Ising model at criticality, which are known to realize higher central charge CFTs [30, 34–37].

Let us consider a Hamiltonian of the general form

$$H = H_{Ising} + \lambda H_{def}. \quad (30)$$

The  $\lambda$  deformation must be Kramers-Wannier invariant in order to not induce a mass gap in the model. For large enough  $\lambda$  this deformation leads to a CFT that contains the Ising symmetries, leading to a higher central charge. There are two deformations that are known to be UV complete

[37], the first is achieved by setting

$$H_{def} = \sum_i X_{i-1} X_i Z_{i+1} + Z_{i-1} X_i X_{i+1}, \quad (31)$$

which leads to the tri-critical Ising CFT with  $c = 7/10$ , for strong  $\lambda$ . Furthermore, we may also set

$$H_{def} = \sum_i Z_i Z_{i+1} + X_{i-1} X_{i+1}, \quad (32)$$

which leads to a  $c = 3/2$  CFT for sufficiently large  $\lambda$ .

In contrast to the Hamiltonians (31) and (32), the  $ZZ$  term alone found in the holographic Hamiltonian explicitly breaks Kramers-Wannier self duality, a hallmark of the Ising criticality that must be included in a UV CFT. Hence, for  $\beta$  sufficiently high at the red critical line in Fig. 7, the holographic Hamiltonian may not be conformally invariant.

To investigate this possibility, we compute the holographic model's central charge as a function of beta along the critical line (29). To do so, we obtain the holographic Hamiltonian ground state by performing a DMRG simulation using the standard ITensor library [38] for varying values of  $\beta$  and system size. For the largest,  $L = 500$ , the simulation's truncation error was kept  $\leq 10^{-10}$  and after 30 sweeps the ground state energy converged to at least 11 significant digits.

To extract an effective central charge, we fit the ground state entanglement entropy to the Calabrese-Cardy scaling formula appropriate for system with periodic boundary [39],

$$S(\ell) = \frac{c}{3} \log \left[ \frac{L}{\pi} \sin \frac{\pi \ell}{L} \right], \quad (33)$$

where  $\ell$  is the subsystem size. This general entanglement scaling is expected when the model admits a low-energy conformal description and the correlation length is large compared to the lattice spacing. In the following, we interpret the extracted central charge as an effective measure of conformal entanglement scaling, rather than as evidence for an exact CFT. The resulting plot for the fitted  $c(\beta)$  for varying system sizes can be found in Fig. 8.

The behavior of the holographic central charge along the critical line is highly non-monotonic. As  $\beta$  increases, the central charge is suppressed near the bulk critical point  $\beta_c$ , before being restored to its original, undeformed value at strong coupling. This behavior suggests that the holographic central charge is primarily sensitive to the presence of bulk gaplessness, rather than serving as a direct indicator of bulk topological order.

The suppression of  $c(\beta)$  admits a natural interpretation in light of a recent work [15], which argues that the bulk phase transitions proceeds through an intermediate gapless phase rather than a direct transition from a topological phase to a trivial gapped phase. In this scenario, the bulk gap

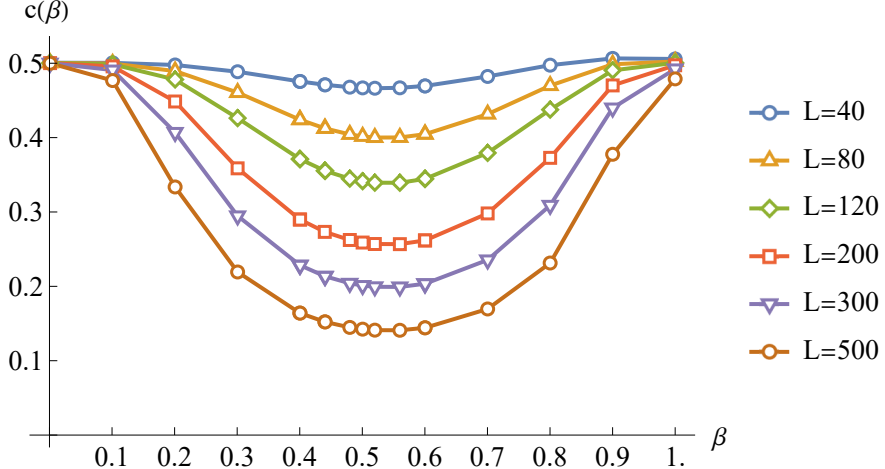


FIG. 8. Plot for  $c(\beta)$  with varying system sizes obtained by fitting the Calabrese-Cardy formula.

closes at  $\beta_c$  and extended critical modes dominate over a finite parameter range. The collapse of the holographic central charge in this region can be understood as a boundary manifestation of this gapless intermediate regime, where the assumptions underlying a simple conformal entanglement scaling break down.

Away from the critical region, the restoration of the holographic central charge indicates the re-emergence of a stable boundary conformal description once the bulk is gapped again. Importantly, this restoration occurs even though the bulk topological entanglement entropy vanishes for  $\beta > \beta_c$ , demonstrating that the recovery of  $c$  does not signal the reappearance of bulk topological order. Instead, it reflects the fact that both gapped phases are characterized by a finite bulk correlation length.

From this perspective, the holographic central charge is controlled by the presence or absence of long-range critical correlations in the bulk. In the vicinity of  $\beta_c$ , the divergence of the bulk correlation length associated with the gapless regime invalidates a simple Calabrese–Cardy scaling of the boundary entanglement entropy, leading to a strong suppression of the effective central charge extracted from finite-size data. Once the bulk gap reopens on either side of the transition and correlations become short-ranged, the entanglement scaling stabilizes and the central charge is restored to its undeformed value.

## VI. FINAL REMARKS

We studied the Castelnovo-Chamon deformation of the toric code from a symmetry and boundary approach. The deformation introduces a controllable string tension that suppresses large loop

configurations and ultimately destroys the  $\mathbb{Z}_2$  topological order above the critical coupling  $\beta_c$ . In the bulk, this loss is sharply reflected by the vanishing of the topological entanglement entropy, while in the presence of open boundaries it is accompanied by a reorganization of its *global* 1-form symmetry operators.

Placing the model on a cylinder allowed us to track how the ordinary toric code boundary condensation and 1-form symmetry breaking are affected by the deformation. At the fixed-point boundaries, the usual toric code picture is recovered: one 1-form symmetry remains unbroken while the anomalous partner is spontaneously broken, leading to the characteristic ground-state degeneracy. Turning on  $\beta$  modifies this structure in an essential way. In particular, the deformed magnetic line operator becomes effectively non-unitary on the ground states beyond  $\beta_c$ , and the associated “magnetic” higher-form *global* symmetry is spontaneously broken. From this viewpoint, the transition is not just an exchange of electric and magnetic roles (as in the  $\beta = 0$  boundary transition), but a genuine destruction of the symmetry and anomaly structure that stabilizes long-range entanglement in the topological phase.

We also examined the transition through a holographic boundary description, where bulk topological lines descend to global symmetries of an effective (1+1)-dimensional Hamiltonian. Along the corresponding boundary critical line, we extracted an effective central charge from DMRG data and found a striking non-monotonic dependence on  $\beta$ . The central charge is strongly suppressed near the bulk critical region and later returns to its undeformed value at larger  $\beta$ . This reinforces the interpretation that the boundary entanglement scaling is primarily sensitive to bulk criticality (or bulk gaplessness) rather than serving as a direct order parameter for bulk topological order.

Several directions remain open. A key problem is to better characterize the intermediate  $\beta_c$ , gapless regime, proposed in [15], and to reconcile it with the symmetry and entanglement scaling diagnostics used here. It would also be valuable to track the fate of electromagnetic duality across the transition more sharply, both in the bulk and on the boundary. Finally, extending these ideas to other deformations, other gauge groups, and more generic perturbations would help clarify which aspects of the “symmetry structure collapse” are special to this exactly solvable model and which are universal mechanisms for the destruction of topological order.

## VII. ACKNOWLEDGMENTS

I would like to thank Dr. Weslei Fontana for the invaluable discussions.

---

[1] Heidar Moradi, Seyed Faroogh Moosavian, and Apoorv Tiwari. Topological holography: Towards a unification of landau and beyond-landau physics. *SciPost Physics Core*, 6(4):066, 2023.

[2] John McGreevy. Generalized symmetries in condensed matter. *Annual Review of Condensed Matter Physics*, 14(1), 2023.

[3] L Bhardwaj, LE Bottini, D Pajer, and S Schafer-Nameki. Categorical landau paradigm for gapped phases, arxiv e-prints. *arXiv preprint arXiv:2310.03786*, 2023.

[4] Ryan Thorngren and Yifan Wang. Fusion category symmetry. part i. anomaly in-flow and gapped phases. *Journal of High Energy Physics*, 2024(4):1–42, 2024.

[5] A Yu Kitaev. Fault-tolerant quantum computation by anyons. *Annals of physics*, 303(1):2–30, 2003.

[6] Claudio Castelnovo and Claudio Chamon. Quantum topological phase transition at the microscopic level. *Physical Review B*, 77(5):054433, 2008.

[7] Joe Huxford, Dung Nguyen, and Yong Baek Kim. Gaining insights on anyon condensation and 1-form symmetry breaking across a topological phase transition in a deformed toric code model. *SciPost Physics*, 15(6):253, 2023.

[8] Brian Swingle, John McGreevy, and Shenglong Xu. Renormalization group circuits for gapless states. *Phys. Rev. B*, 93:205159, May 2016.

[9] Claudio Castelnovo, Claudio Chamon, Christopher Mudry, and Pierre Pujol. From quantum mechanics to classical statistical physics: Generalized rokhsar–kivelson hamiltonians and the “stochastic matrix form” decomposition. *Annals of Physics*, 318(2):316–344, August 2005.

[10] Pedro RS Gomes. An introduction to higher-form symmetries. *SciPost Physics Lecture Notes*, page 074, 2023.

[11] F. J. Wegner. Duality in Generalized Ising Models and Phase Transitions Without Local Order Parameters. *J. Math. Phys.*, 12:2259–2272, 1971.

[12] John Kogut and Leonard Susskind. Hamiltonian formulation of wilson’s lattice gauge theories. *Phys. Rev. D*, 11:395–408, Jan 1975.

[13] John B. Kogut. An introduction to lattice gauge theory and spin systems. *Rev. Mod. Phys.*, 51:659–713, Oct 1979.

[14] Kenneth G. Wilson. Confinement of quarks. *Phys. Rev. D*, 10:2445–2459, Oct 1974.

[15] Rahul Sahay, Curt von Keyserlingk, Ruben Verresen, and Carolyn Zhang. Enforced gaplessness from states with exponentially decaying correlations, 2025.

- [16] Wen-Tao Xu, Tibor Rakovszky, Michael Knap, and Frank Pollmann. Entanglement properties of gauge theories from higher-form symmetries. *arXiv preprint arXiv:2311.16235*, 2023.
- [17] Jiarui Zhao, Zheng Yan, Meng Cheng, and Zi Yang Meng. Higher-form symmetry breaking at ising transitions. *Physical Review Research*, 3(3):033024, 2021.
- [18] Yuji Hirono, Minyoung You, Stephen Angus, and Gil Young Cho. A symmetry principle for gauge theories with fractons. *SciPost Physics*, 16(2):050, 2024.
- [19] Maissam Barkeshli, Yu-An Chen, Po-Shen Hsin, and Ryohei Kobayashi. Higher-group symmetry in finite gauge theory and stabilizer codes. *SciPost Physics*, 16(4):089, 2024.
- [20] Gustavo M. Yoshitome, Heitor Casasola, Rodrigo Corso, and Pedro R. S. Gomes. Generalized modulated symmetries in Z2 topological ordered phases. *Phys. Rev. B*, 112(11):115139, 2025.
- [21] Michael Levin. Protected edge modes without symmetry. *Phys. Rev. X*, 3:021009, May 2013.
- [22] Tsuf Lichtman, Ryan Thorngren, Netanel H. Lindner, Ady Stern, and Erez Berg. Bulk anyons as edge symmetries: Boundary phase diagrams of topologically ordered states. *Phys. Rev. B*, 104(7):075141, 2021.
- [23] Martin Weigel, Lev Barash, Lev Shchur, and Wolfhard Janke. Understanding population annealing monte carlo simulations. *Physical Review E*, 103(5):053301, 2021.
- [24] Jonathan Machta. Population annealing with weighted averages: A monte carlo method for rough free-energy landscapes. *Physical Review E—Statistical, Nonlinear, and Soft Matter Physics*, 82(2):026704, 2010.
- [25] Arkya Chatterjee and Xiao-Gang Wen. Holographic theory for continuous phase transitions: Emergence and symmetry protection of gaplessness. *Phys. Rev. B*, 108:075105, Aug 2023.
- [26] Gregory W. Moore and Nathan Seiberg. Taming the conformal zoo. *Phys. Lett. B*, 220:422–430, 1989.
- [27] Gregory Moore and Nicholas Read. Nonabelions in the fractional quantum hall effect. *Nuclear Physics B*, 360(2-3):362–396, 1991.
- [28] Xiao-Gang Wen. *Quantum Field Theory of Many-Body Systems: From the Origin of Sound to an Origin of Light and Electrons*. Oxford University Press, 09 2007.
- [29] Remember that  $y$  is a boundary parameter and the bulk topological ordering should not depend on a specific choice of  $y$ .
- [30] Kevin Slagle, David Aasen, Hannes Pichler, Roger SK Mong, Paul Fendley, Xie Chen, Manuel Endres, and Jason Alicea. Microscopic characterization of ising conformal field theory in rydberg chains. *Physical Review B*, 104(23):235109, 2021.
- [31] Eran Sela and Rodrigo Gonçalves Pereira. Orbital multicriticality in spin-gapped quasi-one-dimensional antiferromagnets. *Physical Review B—Condensed Matter and Materials Physics*, 84(1):014407, 2011.
- [32] Hosho Katsura, Dirk Schuricht, and Masahiro Takahashi. Exact ground states and topological order in interacting kitaev/majorana chains. *Physical Review B*, 92(11):115137, 2015.
- [33] Fabian Hassler and Dirk Schuricht. Strongly interacting majorana modes in an array of josephson junctions. *New Journal of Physics*, 14(12):125018, 2012.

- [34] Armin Rahmani, Xiaoyu Zhu, Marcel Franz, and Ian Affleck. Phase diagram of the interacting majorana chain model. *Physical Review B*, 92(23):235123, 2015.
- [35] Shouvik Datta and Yunfeng Jiang.  $t\bar{t}$  deformed partition functions. *Journal of High Energy Physics*, 2018(8):1–22, 2018.
- [36] Luca Griguolo, Rodolfo Panerai, Jacopo Papalini, and Domenico Seminara. The phase diagram of  $t\bar{t}$ -deformed yang-mills theory on the sphere. *Journal of High Energy Physics*, 2022(11):1–25, 2022.
- [37] André LeClair.  $t\bar{t}$  deformation of the ising model and its ultraviolet completion. *Journal of Statistical Mechanics: Theory and Experiment*, 2021(11):113104, 2021.
- [38] Matthew Fishman, Steven White, and Edwin Miles Stoudenmire. The itensor software library for tensor network calculations. *SciPost Physics Codebases*, page 004, 2022.
- [39] Pasquale Calabrese and John Cardy. Entanglement entropy and quantum field theory. *Journal of statistical mechanics: theory and experiment*, 2004(06):P06002, 2004.